Cu(II) ion coordination to SPARC: a model study on short peptide fragments

Maurizio Remelli,*[a] Marek Łuczkowski,[b] Arkadiusz Mieczysław Bonna,[c] Zbigniew Mackiewicz,[c] Chiara Conato[a] and Henryk Kozłowski*[b]

[a] *Dipartimento di Chimica, Università di Ferrara, Via L. Borsari 46, I-44100, Ferrara, Italia. E-mail: rmm@unife.it; Fax: +39 0532 240709*
[b] *Faculty of Chemistry, University of Wrocław, F. Joliot-Curie 14, 50-383, Wrocław, Poland. E-mail: henrykoz@wchuwr.chem.uni.wroc.pl*
[c] *Faculty of Chemistry, University of Gdansk, Sobieskiego 18/1, 80-952, Gdańsk, Poland*

Received (in Montpellier, France) 9th July 2002, Accepted 15th October 2002
First published as an Advance Article on the web 2nd January 2003

SPARC (**s**ecreted **p**rotein, **a**cidic and **r**ich in **c**ysteine) is a glycoprotein of the extracellular matrix that mediates the cell-matrix interactions. It plays also a role in angiogenesis, tumorigenesis, caractogenesis and wound healing. The human SPARC consists of three distinct modules. Module II is follistatin-like and its hydrolysis gives rise to a number of oligopeptides that can regulate angiogenesis *in vivo* and the biological activity of which has been related to their association with endogenous or exogenous copper ion.

In order to completely understand the biological role of metal complexes formed by SPARC and its fragments, more information is needed on their stoichiometry, stability and structure in solution. In the present paper a potentiometric and spectroscopic investigation on Cu(II) complexes with the three $SPARC_{122–126}$, $SPARC_{121–126}$ and $SPARC_{120–126}$ fragments, protected at both their amino and carboxylic ends, is reported. These peptides (Ac-HKLHL-NH_2, Ac-GHKLHL-NH_2 and Ac-KGHKLHL-NH_2, respectively) constitute good models for the strong copper-binding site of the protein.

The behaviour of the three ligands is very similar: complex formation is started by the two His residues, subsequently involving up to three amido nitrogens, as pH increases. The coordination of the two histydyl imidazoles promotes amide ionization in the physiological pH range and this can explain SPARC binding to the Cu(II) ion.

SPARC (**s**ecreted **p**rotein, **a**cidic and **r**ich in **c**ysteine), also known as osteonectin or BM-40, is a 32 kD calcium-binding protein of the extracellular matrix. It is secreted by many different types of cells and belongs to the class of "matricellular" proteins.[1] It mediates the cell-matrix interactions without playing any primarily structural role:[2,3] it has counter-adhesive properties, it modulates the activity of some growth factors and it influences the cell cycle. SPARC is the product of a single-copy gene and its sequence has been highly conserved during vertebrate evolution and among species.[4] SPARC is highly expressed during embryonic development; its expression in the adult is instead associated with tissue remodelling or renewal, also during wound healing. It has also been reported that SPARC production is increased in some tumours[5] and SPARC has been proposed as a diagnostic marker of invasive meningiomas.[6] These findings have been associated to the activity of SPARC and of its fragments in angiogenesis,[7] the latter being a fundamental requirement for tumour development. A high angiogenic activity in turn requires high levels of copper, whose the reduction in the body has been recently suggested as a therapeutic tool to control cancer growth.[8] In this context, the interactions between the copper ion and the SPARC protein (and its fragments) assume a particular interest.

The human protein consists of 286 amino acids, belonging to three distinct modules; the structure of the last two modules is known.[9] The N-terminal module (residues 1–52, after a 17 amino acid signal sequence) is an acidic region, which binds 5–8 calcium ions with low affinity. It interacts with hydroxyapatite, being involved in the mineralization of cartilages and bones. Invertebrate SPARC does not have this ability, developed for a specific function particular to vertebrates, that is bone formation. The second module is a Cys-rich, follistatin-like domain (residues 53–137), in which all the 10 Cys residues are disulfide-bonded. A carbohydrate moiety is N-linked at Asn_{99}. This module contains two bioactive peptides (peptide 2.1, residues 55–74; peptide 2.3, residues 114–130), which proved to be responsible for the SPARC ability to bind the copper ion.[10] The latter fragment, corresponding to the strongest Cu(II)-binding site of the protein, contains the sequence Gly-His-Lys (GHK) (residues 121–123). GHK, better known as a liver-cell growth factor,[11] is a well recognized Cu(II) binding peptide;[12] it is present in the human serum and it most likely derives from SPARC hydrolysis.[10] Cu(II)–GHK complexes proved to have angiogenic activity and to play an important role in wound healing.[11] Module III (residues 138–286) is largely α-helical and contains the extracellular high-affinity calcium binding sites. It is globular and contains two EF-hand motifs.

The complex formation equilibria of Ac-TLEGTKK-GHKLHLDY-NH_2—corresponding to the $SPARC_{114–128}$ fragment—with the Cu(II) has been recently investigated.[13] The involvement of His_{122} and His_{125} in the Cu(II) complex formation has been suggested. The promoted-by-copper deprotonation of at least three neighbouring amido nitrogens has been reported, as well. In order to better clarify the role played by each peptide residue, in the present paper the Cu(II) complex formation equilibria of the three $SPARC_{122–126}$ (Ac-HKLHL-NH_2), $SPARC_{121–126}$ (Ac-GHKLHL-NH_2) and

$SPARC_{120–126}$ (Ac-KGHKLHL-NH_2) fragments, protected at both their amino and carboxylic ends, have been investigated, at $I = 0.1$ mol dm^{-3} (KNO_3) and $T = 298.2$ K. Protonation and complex formation constants were potentiometrically determined; formation enthalpies have been measured by direct solution calorimetry; complex formation model and species stoichiometry have been carefully checked by means of UV-VIS absorption, CD and EPR spectroscopies. Hypotheses on the structure of the complex species are suggested.

Experimental

Synthesis of the ligands

Starting materials. N^{α}-9-Fluorenylmethyloxycarbonyl amino acids were obtained from Bachem, trifluoroacetic acid (TFA), 1,3-diisopropylcarbodiimide (DIC), piperidine, *N*-hydroxybenzotriazole (HOBt), Triton, triisopropylsilane (TIS), dimethylformamide (DMF), *N*-methyl-2-pyrolidone (NMP), methylene chloride (DCM), and acetonitrile (HPLC grade) were purchased from Fluka AG. All solvents and reagents used for solid-phase syntheses were of analytical grade. TentaGel resin S RAM was obtained from Rapp Polymere.

Synthesis of the peptides. The peptides were synthesized manually by the solid-phase method using the Fmoc/Bu^t procedure.[14] The side-chain protecting groups of the amino acids were Boc for Lys and trityl for His. All peptides were synthesized using the Fmoc method, according to the following procedure: (*i*) 5 and 15 min deprotection steps using 33% piperidine in DMF; (*ii*) the coupling reactions carried out with the protected amino acid diluted in a mixture of DMF–*N*-methylpirrolidone (1:1, v/v) in the presence of 1% Triton using DIC as the coupling reagent in the presence of HOBt (Fmoc-AA:DIC:HOBt; 1:1:1) for 1 h. The completeness of each coupling reaction was monitored by the chloranil test.[15] The protected peptidyl resins were treated with a mixture of 95% TFA, 2.5% water and 2.5% TIS for 1.5 h. The cleaved peptide was precipitated with diethyl ether and lyophilized.

Purification of peptides. Peptides were purified by solid-phase extraction (SPE), as previously described.[16] The purity of the products was tested by reversed-phase high performance liquid chromatography (RP-HPLC). RP-HPLC was performed on a Beckman System Gold chromatograph with Knauer column (5 μm particle size, 4.6 × 250 mm), flow rate was 1 ml min^{-1}, absorbance at 226 nm. The mobile buffer consisted of (A) 0.1% TFA in water and (B) 0.1% TFA in acetonitrile. The peptides were characterized with a linear gradient 5–80% of B for 20 min. Fractions containing pure peptides (> 95%) were pooled and lyophilized.

The synthesized peptides showed the right molecular mass, measured by the FAB-MS technique. The mass spectra were obtained on an AMD-604 spectrometer. The ion source was equipped with a Cs^+ gun and the energy of the Cs^+ ions was 12 keV.

Measurements

Potentiometric titrations. Aliquots (2.5 cm^3) of sample solution, containing suitable amounts of the metal ion, one of the ligands, HNO_3 (when the initial pH value needed to be lowered) and KNO_3 (to adjust the ionic strength to 0.1 mol dm^{-3}) were potentiometrically titrated with standard NaOH in a thermostatted potentiometric vessel (pH range = 3.5–11.0; $T = 298.2$ K). Metal ion concentration was close to 1×10^{-3} mol dm^{-3} and the metal-to-ligand ratio was 1:1.2. Two pairs of potentiometric titrations, both for protonation and complex formation, were performed. Further experimental details, equipment and software used are reported elsewhere.[17] Throughout, species stabilities are reported either as step or cumulative constants (K and β, respectively), the latter referring to the overall equilibrium: $p\mathrm{M} + q\mathrm{L} + r\mathrm{H} = \mathrm{M}_p\mathrm{L}_q\mathrm{H}_r$.

Spectroscopic measurements. CD, EPR and UV-VIS spectra were recorded on a JASCO J 715, on a Bruker ESP 300E (at 120 K and 9.4 GHz) and on a Beckman DU 650 spectrometer, respectively. Sample solutions had the same composition as above; pH was varied by addition of suitable amounts of standard NaOH or HCl, under potentiometric control. Spectra every 0.5 pH units were recorded.

Calorimetric measurements. Calorimetric titrations were performed by means of an Isoperibolic Calorimeter (Tronac) at 298.2 K, by addition of standard HNO_3 to a sample solution (2.5 cm^3) of the same composition as above. For each system two pairs of calorimetric titrations containing not less than 250 experimental points were utilized to calculate the thermodynamic quantities, as previously described.[7] Thermodynamic data are given with the estimated accuracy reported as the uncertainty on the last significant figure.

Results

Ligand protonation

The title ligands contain some basic side groups, the imidazole rings of His_{122} and His_{125} and the ε-amino group of Lys_{123} (and of Lys_{120} in the case of Ac-KGHKLHL-NH_2). The thermodynamic parameters reported in Table 1 are in good agreement with the available literature data.[18,19] Comparing the results obtained with different chain lengths and taking also into account previous results on the $SPARC_{114–128}$ fragment[13] it is possible to tentatively assign a log$K$ value to each residue. The highest log$K$ values (9.8–10.5) are certainly due to the amino side groups of Lys residues. In the case of Ac-KGHKLHL-NH_2 the thermodynamic parameters corresponding to the second deprotonation step (log$K$ = 9.82; $\Delta H^\circ = 27$ kJ mol^{-1}) are in good agreement with those of the other two ligands, suggesting that this step should be due to the Lys_{123} residue. Moreover, it can be observed that the lowest imidazole log$K$ (5.6–5.9) steadily increases by addition of new amino acid residues at the N-terminal; on the contrary, the second imidazole log$K$ (6.6–6.7) remains approximately constant. The same is true for the corresponding ΔH° values, as well. As a consequence, the latter pK value can be ascribed to His_{125},

Table 1 Thermodynamic parameters for ligand protonation at 298.2 K and $I = 0.1$ mol dm^{-3} (KNO_3). Estimated accuracy is in parentheses

	Ac-HKLHL-NH_2				Ac-GHKLHL-NH_2				Ac-KGHKLHL-NH_2			
Residue	log K	$-\Delta G^\circ$/ kJ mol^{-1}	$-\Delta H^\circ$/ kJ mol^{-1}	ΔS°/ J mol^{-1} K^{-1}	log K	$-\Delta G^\circ$/ kJ mol^{-1}	$-\Delta H^\circ$/ kJ mol^{-1}	ΔS°/ J mol^{-1} K^{-1}	log K	$-\Delta G^\circ$/ kJ mol^{-1}	$-\Delta H^\circ$/ kJ mol^{-1}	ΔS°/ J mol^{-1} K^{-1}
Lys_{120}									10.49 (2)	59.8 (1)	68 (4)	−29 (15)
Lys_{123}	10.29 (3)	58.7 (2)	26 (3)	110 (10)	10.15 (3)	57.9 (2)	34 (2)	82 (8)	9.82 (1)	56.1 (1)	27 (3)	40 (12)
His_{125}	6.66 (5)	38.0 (3)	31 (3)	23 (9)	6.66 (3)	38.0 (2)	31 (2)	22 (8)	6.58 (2)	37.5 (1)	32 (4)	18 (15)
His_{122}	5.62 (9)	32.1 (5)	17 (2)	50 (7)	5.79 (2)	33.0 (1)	26 (2)	23 (6)	5.86 (4)	33.4 (2)	22 (4)	39 (16)

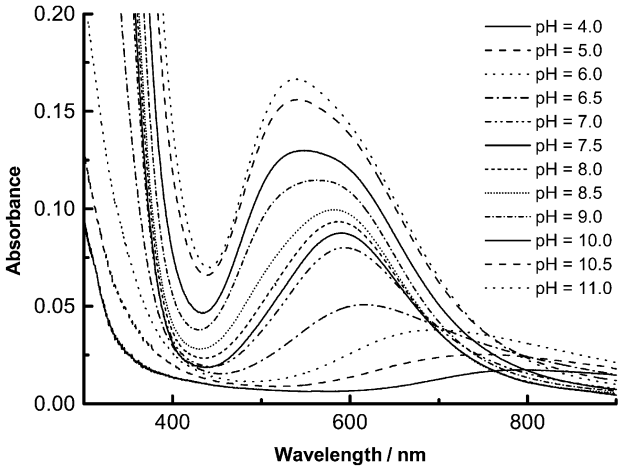

Fig. 1 Absorption spectra of Cu(II)–Ac-GHKLHL-NH_2 solutions. [Cu(II)] = 1.0×10^{-3} mol dm^{-3}, [Ac-GHKLHL-NH_2] = 1.2×10^{-3} mol dm^{-3}, T = 298.2 K, I = 0.1 mol dm^{-3} (KNO_3).

the most distant His residue from the N-terminal. A deeper investigation on this topic, through the NMR determination of the corresponding microconstants, is beyond the aim of the present work. In fact, in the presence of Cu(II) ions, the small difference in basicity between the analogous residues cannot significantly influence the complexation behaviour of the ligands.

Copper complexes

The three ligands essentially behave in the same manner towards the copper ion, as can be inferred by the similarity of the experimental results described below. Sample solutions containing Cu(II) ions and one of the ligands—in a nearly equimolar amount—were pale-blue coloured at acidic pH, violet at neutral pH and purple in the most basic pH region. This behaviour is reflected in the variation of both position and intensity of the VIS spectra, showing the typical "blue-shift" as pH increases. An example is shown in Fig. 1 while the whole set of spectroscopic results is reported in Table 2. VIS spectra are dominated by three main absorption bands whose intensity depends on pH. The first is located around 685 nm and prevails at acidic pH; the second has its maximum at 580–600 nm and prevails around neutrality; the third, the most intense, is located at 520–530 nm and dominates in the alkaline pH range.

The CD spectra show four distinct absorption bands (Fig. 2 and Table 2). A double band is present in the d-d region, from pH 6 on, which is typical of Cu(II)–His coordination.[20] The two bands at 250–260 (positive) and at 340–360 nm (negative) can be ascribed to a charge transfer (CT) transition from imidazole π_2 and π_1 to copper, respectively.[21] The positive band at 314–322 nm is most likely due a CT transition from a deprotonated amidic nitrogen to copper.[21]

The $A_{\parallel}$ and $g_{\parallel}$ parameters of the EPR spectra are reported in Table 2. At pH = 6 they assume the typical values of a 2N complex[22] and at pH = 7–8 those of a 3N complex.[22] In the pH range 8.5–9.5, $A_{\parallel}$ increases while $g_{\parallel}$ slightly decreases, suggesting the coordination of a further N atom; from pH 9.5 EPR data are typical of a 4N complex characterized by a strong ligand field.[22] A further increase of solution pH does not cause any change in the EPR spectra.

The complete set of thermodynamic complex formation data is reported in Table 3. As the distribution diagrams of Fig. 3 show, complex formation starts below pH 4; at neutral pH all the Cu(II) ion is involved in complexation.

Up to seven mono complexes are formed by the three ligands, with a variable degree of protonation. It is worth noting that the longest peptide (Ac-KGHKLHL-NH_2) contains an additional amino side group (in the first Lys residue), which is protonated at pH lower than 9. This difference must be taken into account when comparing the three binary metal-ligand systems at acidic or neutral pH.

The acidic pH range is dominated by a complex where the ligand has lost two protons and it most likely behaves as a bidentate ligand. The other two protons are lost in a very narrow pH range, thus forming the most important species at neutral pH (MLH_{-1} for Ac-HKLHL-NH_2 and Ac-GHKLH-NH_2; ML for Ac-KGHKLHL-NH_2). A further proton is lost between pH 8 and 9 leading to the species that dominates the alkaline pH range. Finally, above pH 9, other protons are lost and the corresponding log$K$ values are quite similar to that of the Lys residues in the free ligands (see Table 1).

Discussion

First of all is worth noting that all the ligands are protected at both their N- and C-terminals, which instead usually take part

Table 2 Spectroscopic parameters for the most important Cu(II) complexes at 298.2 K and I = 0.1 mol dm^{-3} (KNO_3)

pH	Main species	UV-VIS λ/nm (ε/M^{-1} cm^{-1})	CD λ/nm ($\Delta\varepsilon$/M^{-1} cm^{-1})	EPR $A_{\parallel}$/G; $g_{\parallel}$
Cu(II)–Ac-HKLHL-NH_2				
6.0	MLH	691 (41)	642 (−0.04); 254 (0.38)	164; 2.31
7.0	ML	653 (63)	609 (−0.10); 528 (0.06); 352 (−0.09); 253 (1.80)	164; 2.27
7.5	MLH_{-1}	608 (122)	659 (0.07); 575 (−0.12); 482 (−0.29); 360 (−0.27); 318 (0.42); 250 (4.72)	168; 2.21
9.0	MLH_{-2}	521 (155)	649 (0.39); 492 (−0.87); 365 (−0.24); 322 (1.03); 252 (4.95)	195; 2.19
11.0	MLH_{-3}	519 (146)	652 (0.67); 499 (−1.26); 356 (−0.46); 318 (0.73); 258 (6.38)	195; 2.19
Cu(II)–Ac-GHKLHL-NH_2				
6.0	MLH	685 (31)	250 (0.35)	160; 2.31
7.5	MLH_{-1}	601 (72)	646 (−0.03); 529 (0.33); 338 (−0.16); 253 (3.41)	177; 2.23
9.5	MLH_{-2}	524 (92)	629 (0.20); 480 (−0.23); 360 (−0.13); 318 (0.37); 253 (4.69)	200; 2.19
10.5	MLH_{-3}	522 (128)	645 (0.43); 490 (−0.69); 360 (−0.39); 318 (0.89); 256 (5.29)	205; 2.18
11.0	MLH_{-4}	520 (141)	661 (0.68); 496 (−1.00); 354 (−0.78); 313 (0.81); 256 (6.79)	195; 2.19
Cu(II)–Ac-KGHKLHL-NH_2				
6.0	MLH_2	688 (49)	546 (0.10); 340 (−0.09); 254 (1.15)	155; 2.32
7.5	ML	608 (107)	548 (0.39); 341 (−0.39); 249 (4.67)	180; 2.23
9.0	MLH_{-1}	520 (129)	616 (0.74); 487 (−0.57); 361 (−0.18); 316 (0.94); 252 (5.39)	200; 2.19
10.0	MLH_{-2}	520 (157)	620 (0.88); 490 (−0.94); 364 (−0.19); 319 (1.41); 253 (5.81)	200; 2.19
11.0	MLH_{-3}	525 (175)	625 (1.11); 493 (−1.35); 359 (−0.38); 316 (1.38); 257 (7.00)	200; 2.19

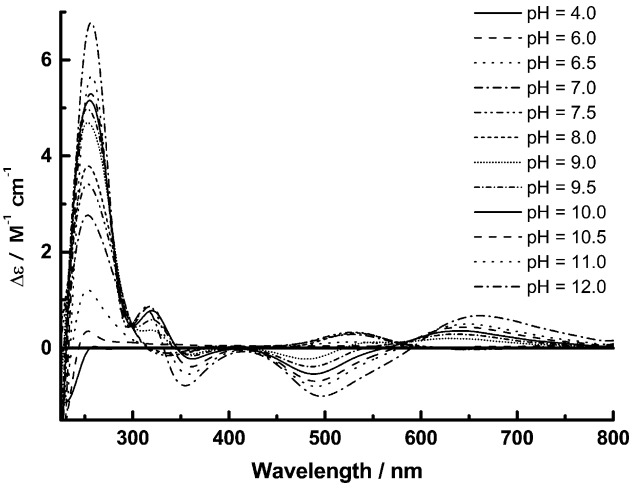

Fig. 2 Circular dichroism spectra of Cu(II)–Ac-GHKLHL-NH_2 solutions. [Cu(II)] = 1.0×10^{-3} mol dm^{-3}, [Ac-GHKLHL-NH_2] = 1.2×10^{-3} mol dm^{-3}, $T = 298$ K, $I = 0.1$ mol dm^{-3} (KNO_3).

in complex formation in the case of unprotected peptides. For this reason any comparison with previously studied systems containing unprotected SPARC fragments (*e.g.*, GHK[11] or KGHK[19]) is meaningless.

The present ligands contain a number of nitrogen atoms constituting potential donor sites to form coordination complexes with the Cu(II) ion. These atoms belong to the imidazole ring of the His residues (N_{Im}), to the peptidic linkages (N^-) and to the ε-amino group of Lys residues (N_{amino}). Among them only N_{Im} is able to bind copper at pHs as low as 4. The first observed species, MLH_2 (in the case of Ac-HKLHL-NH_2 and Ac-GHKLHL-NH_2), should be a complex where the ligand binds the metal ion in a monodentate fashion, by means of one of its N_{Im} atoms (1N species). Both of the His residues can perform this complexation and a mixture of two hardly distinguishable species is most likely present in solution. Due to the proximity of the two His residues and to the similarity of their protonation log*K*s, the bound-to-copper ligand readily loses a further proton. The distribution diagrams (Fig. 3) show that the 1N complex forms in only very small amounts and it even could not be detected in the case of Ac-KGHKLHL-NH_2.

The next complex to be formed (MLH in the case of Ac-HKLHL-NH_2 and Ac-GHKLHL-NH_2; MLH_2 in the case of Ac-KGHKLHL-NH_2) is the main species in the acidic pH range. The corresponding deprotonation log*K* (~4) is compatible with the deprotonation and coordination of the second His residue (2N species). Both the wavelength of maximum absorption in the VIS spectra and the EPR parameters agree with the above hypothesis (see Table 2).[22,23] In the CD spectra the band at 250–260 nm becomes more and more intense as pH increases, while the $N_{Im} \rightarrow Cu\ \pi_1$ CT transition band (340–360 nm) starts to be detectable at pH 6.0–6.5. The corresponding enthalpy values, once corrected for the contribution due to Lys protonation, assume a value of 41–46 kJ mol^{-1}, supporting the hypothesis of two N_{Im} atoms bound to copper. A structural hypothesis for this complex is shown in Fig. 4: the two imidazole rings are bound in the equatorial plane of the complex and two carbonyl (or water) oxygens occupy the other two positions of the plane.

When pH is raised from 6.0 to 8.0 two additional protons are lost in quick sequence. The MLH_{-1} species (ML in the case of Ac-KGHKLHL-NH_2) is formed: it is the main species in the neutral and slightly alkaline pH range (see distribution diagrams of Fig. 3). The corresponding log*K* values (6.2–7.2, Table 3) suggest that the Cu(II) ion promotes the deprotonation of two amido nitrogens, as already reported in the literature for analogous systems.[13,24–27] The d-d bands in both the CD and VIS spectra shift towards lower wavelengths, suggesting that additional nitrogen atoms bind the metal ion. A first hypothesis could be that the amido nitrogens belonging to the two His residues replace the oxygens bound to copper (see Fig. 4), thus allowing the formation of a 4N complex, characterized by two six-membered chelate rings [Fig. 5(a)]. This change from oxygen to nitrogen donors of the same peptide linkage is common to unprotected peptides.[28] However, both the wavelength of maximum absorption and the EPR parameters measured in the pH range 7.5–8.0 assume typical values corresponding to a 3N Cu(II) complex.[22,23] It is also interesting to observe that the loss of the first proton is especially favoured from the enthalpic point of view while the entropy change is unfavourable for all the present ligands. The same was also reported in the case of the $SPARC_{114–128}$ fragment.[13] This behaviour can be attributed to the presence of additional non-bonding interactions with the formation of an ordered structure. The sum of the above observations suggests the structure hypothesis shown in Fig. 5(b): one of the imidazole nitrogens leaves the equatorial plane and moves towards the axial position, where it can interact with both the Cu(II) ion and with the second His residue, with aromatic ring stacking. The equatorial plane is occupied by the other imidazole along with the two deprotonated amido nitrogens and one oxygen.

Above pH 8.5 a further relevant blue shift can be observed in the VIS spectra where a new band (520 nm) appears and becomes the most intense. This suggest the coordination of an additional nitrogen atom in the equatorial plane of the complex. EPR data in the same pH range lead to the same hypothesis. On the other hand, CD spectra remain approximately the same, with only an increase in the band intensity. Therefore, the nature of the donor centres should not change: imidazole and amido nitrogens. As the distribution diagrams in Fig. 3 show, a new important species dominates the pH 8.5–9.5 range: the complex MLH_{-2} in the case of Ac-HKLHL-NH_2 and Ac-GHKLHL-NH_2 or MLH_{-1} in the case of Ac-KGHKLHL-NH_2. The corresponding log*K* values

Table 3 Thermodynamic parameters for Cu(II) binary complex formation at 298.2 K and $I = 0.1$ mol dm^{-3} (KNO_3). Estimated accuracy is in parentheses

	Ac-HKLHL-NH_2			Ac-GHKLHL-NH_2			Ac-KGHKLHL-NH_2		
Species	log*β*	$-\Delta H°$ / kJ mol^{-1}	$\Delta S°$ / J mol^{-1} K^{-1}	log*β*	$-\Delta H°$ / kJ mol^{-1}	$\Delta S°$ / J mol^{-1} K^{-1}	log*β*	$-\Delta H°$ / kJ mol^{-1}	$\Delta S°$ / J mol^{-1} K^{-1}
MLH_2	20.1 (1)	110 (30)	~0	19.7 (4)	–	–	25.94 (9)	137 (4)	36 (15)
MLH	15.79 (3)	67 (5)	78 (18)	15.85 (4)	78 (4)	43 (14)	19.1 (1)	162 (9)	−177 (33)
ML	8.62 (7)	85 (9)	−120 (38)	8.74 (9)	111 (13)	−206 (42)	12.8 (1)	83 (5)	−34 (17)
MLH_{-1}	1.50 (5)	27 (7)	−61 (27)	2.52 (7)	25 (5)	−35 (17)	4.3 (2)	39 (5)	−49 (19)
MLH_{-2}	−6.62 (8)	−19 (7)	−62 (27)	−5.9 (1)	−19 (5)	−49 (18)	−5.5 (3)	9 (7)	−135 (24)
MLH_{-3}	−16.7 (1)	−43 (9)	−170 (32)	−15.9 (1)	−44 (6)	−155 (21)	−15.9 (3)	−48 (7)	−143 (24)
MLH_{-4}				−27.1 (2)	−99 (10)	−185 (36)			

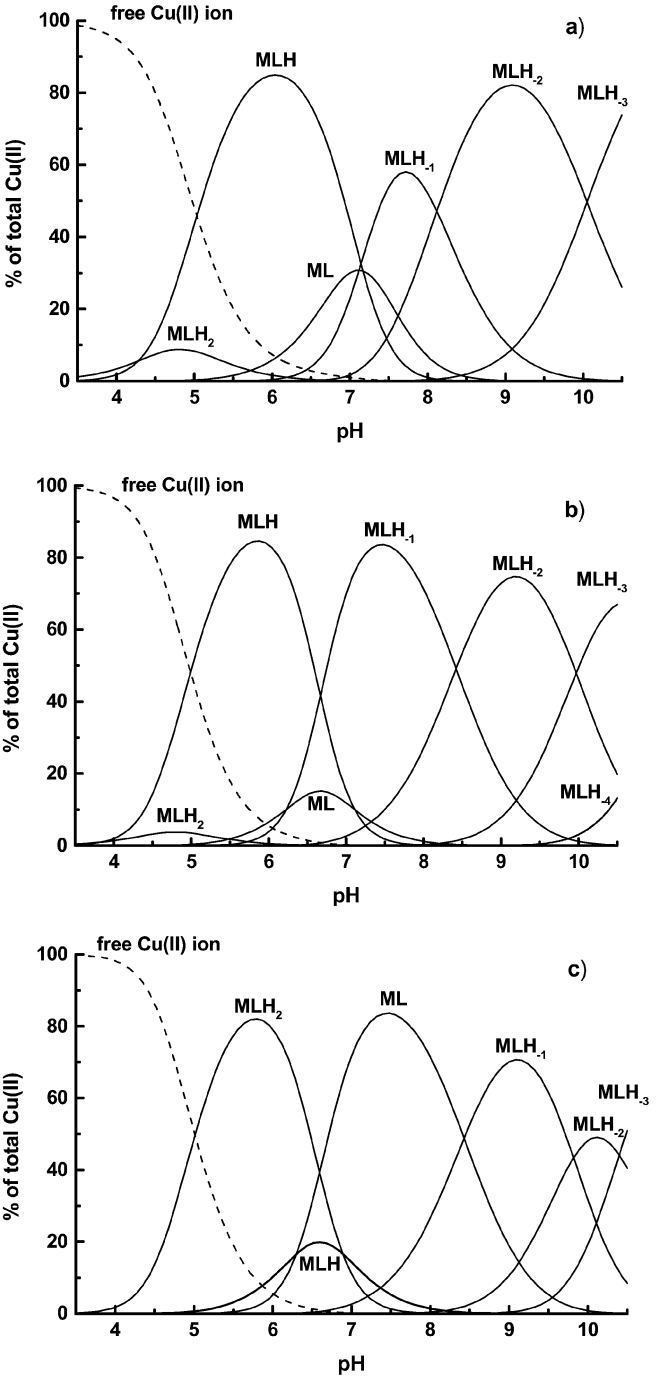

Fig. 3 Distribution diagrams of binary Cu(II) complexes at 298.2 K and $I = 0.1$ mol dm^{-3} (KNO_3), [Cu(II)] = 1.0×10^{-3} mol dm^{-3}, [ligand] = 1.2×10^{-3} mol dm^{-3}. (a) Ac-HKLHL-NH_2; (b) Ac-GHKLHL-NH_2; (c) Ac-KGHKLHL-NH_2.

(8.1–8.4) are compatible with the deprotonation of a further amido nitrogen, promoted by interaction with copper.[29] This process is accompanied by both an enthalpy and entropy loss, as expected. Many hypotheses can be put forward concerning the structure of this complex, since different amido nitrogens are present in the ligands. The investigation on the Cu(II)–$SPARC_{114–128}$ system cited above[13] reported the formation of an analogous complex species in the alkaline pH range, where Lys_{120}, Gly_{121} and His_{122} gave the N^- donor atoms bound in the equatorial plane. The His_{122} imidazole nitrogen occupied the fourth position on the plane while the His_{125} imidazole was interacting with the copper ion in the axial position giving, at the same time, a stacking interaction with the phenol ring of Tyr_{128}. The same coordination behaviour is possible

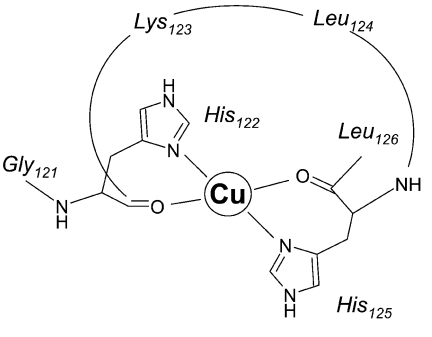

Fig. 4 Structural hypothesis for the Cu(II)–Ac-GHKLHL-NH_2 complex at pH 6.0 (MLH species).

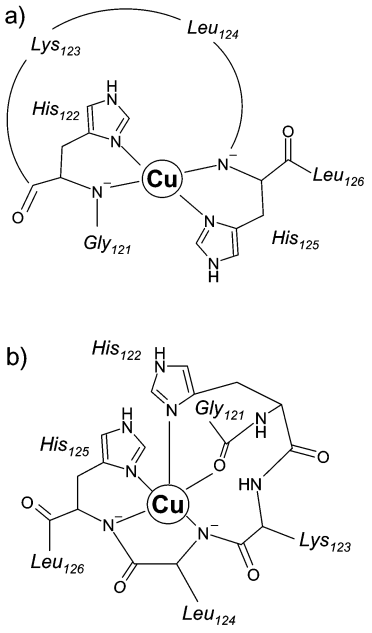

Fig. 5 Structural hypotheses for the Cu(II)–Ac-GHKLHL-NH_2 complex at pH 7.5 (MLH_{-1} species).

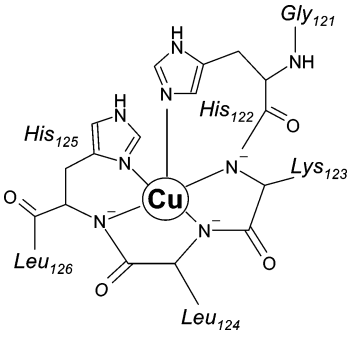

Fig. 6 Structural hypothesis for the Cu(II)–Ac-GHKLHL-NH_2 complex at pH 9.5 (MLH_{-2} species).

here only for the longest fragment (Ac-KGHKLHL-NH_2), without the stacking interaction with Tyr, which is absent. An alternative structure hypothesis, fitting very well all the experimental observations and directly deriving from the complex of Fig. 5(b), is that shown in Fig. 6. In this case, the Lys_{123}, Leu_{124} and His_{125} amido nitrogens and the imidazole ring of the His_{125} residue are equatorially coordinated to copper while His_{122} axially interacts with the metal ion and/or with the other aromatic ring. A very similar structure hypothesis has been recently reported for some protected oligopeptides containing two or more His residues, spaced by Gly residues.[27]

Finally, increasing the pH value, one or two further protons are lost by the complexed ligands. The corresponding log$K$ and ΔH° values are very close to those reported in Table 1 for the Lys residues in the free ligands. Spectral features do not vary in the most alkaline pH range: the involvement in complex formation of these amino side groups does not look very likely. In the case of Ac-GHKLHL-NH_2 a further species is observed, namely the MLH_{-4} complex, characterized by a log$K$ value of 11.2, compatible with pyrrolic nitrogen deprotonation by an imidazole residue already bound to copper.[30]

Acknowledgements

The financial supports by University of Ferrara (ex-60%), Polish State Committee for Scientific Research (KBN 4 T09A 05423) and University of Gdansk (BW-8000-5-0290-2) are gratefully acknowledged.

References

1 P. Bornstein, *Matrix Biol.*, 2000, **19**, 555.
2 R. A. Brekken and E. H. Sage, *Matrix Biol.*, 2000, **19**, 569.
3 A. D. Bradshaw and E. H. Sage, *J. Clin. Invest.*, 2001, **107**, 1049.
4 Q. Yan and E. H. Sage, *J. Histochem. Cytochem.*, 1999, **47**, 1495.
5 T. F. Lane and E. H. Sage, *FASEB J.*, 1994, **8**, 163.
6 S. A. Rempel, S. Ge and J. A. Gutierrez, *Clin. Cancer Res.*, 1999, **5**, 237.
7 E. H. Sage, *Nat. Med. (N. Y.)*, 1997, **3**, 144.
8 G. J. Brewer, *Exp. Biol. Med.*, 2001, **226**, 665.
9 E. Hohenester, P. Maurer and R. Timpl, *EMBO J.*, 1997, **16**, 3778.
10 T. F. Lane, M. L. Iruela-Arispe, R. S. Johnson and E. H. Sage, *J. Cell Biol.*, 1994, **125**, 929.
11 L. Pickart, J. Freedman, W. J. Loker, J. Peisach, C. M. Perkins, R. E. Stenkamp and B. Weinstein, *Nature (London)*, 1980, **288**, 715.
12 C. Conato, R. Gavioli, R. Guerrini, H. Kozłowski, P. Młynarz, C. Pasti, F. Pulidori and M. Remelli, *Biochim. Biophys. Acta*, 2001, **1526**, 199 and references therein.
13 C. Conato, W. Kamysz, H. Kozłowski, M. Łuczkowski, Z. Mackiewicz, P. Młynarz, M. Remelli, D. Valensin and G. Valensin, *J. Chem. Soc., Dalton Trans.*, 2002, 3939.
14 E. Atherton and R. C. Sheppard, in *The Peptides: Analysis, Synthesis, Biology*, eds. S. Udenfriend and J. Meienhofer, Academic Press, New York, 1987, vol. 9, p. 1.
15 W. S. Hancock and J. E. Battersby, *Anal. Biochem.*, 1976, **71**, 260.
16 W. Kamysz, B. Kochańska, A. Kędzia, J. Ochocińska, Z. Maćkiewicz and G. Kupryszewski, *Pol. J. Chem.*, 2002, **76**, 801.
17 M. Remelli, C. Conato, A. Agarossi, F. Pulidori, P. Młynarz and H. Kozłowski, *Polyhedron*, 2000, **19**, 2409.
18 L. D. Pettit and H. K. J. Powell, *The IUPAC Stability Constants Database*, Academic Software and IUPAC, Royal Society of Chemistry, London, 1992–1997.
19 C. Conato, H. Kozłowski, P. Młynarz, F. Pulidori and M. Remelli, *Polyhedron*, 2002, **21**, 1469.
20 P. Młynarz, W. Bal, T. Kowalik-Jankowska, M. Stasiak, M. T. Leplawy and H. Kozłowski, *J. Chem. Soc., Dalton Trans*, 1999, 109.
21 P. G. Daniele, E. Prenesti and G. Ostacoli, *J. Chem. Soc., Dalton Trans.*, 1996, 3269.
22 J. Peisach and W. E. Blumberg, *Arch. Biochem.*, 1974, **165**, 691.
23 H. Sigel and R. B. Martin, *Chem. Rev.*, 1982, **82**, 385.
24 L. D. Pettit, S. Pyburn, W. Bal, H. Kozłowski and M. Bataille, *J. Chem. Soc., Dalton. Trans.*, 1990, 3565.
25 M. A. Zoroddu, M. Peana, T. Kowalik-Jankowska, H. Kozłowski and M. Costa, *J. Chem. Soc., Dalton. Trans.*, 2002, 458.
26 M. Casolaro, M. Chelli, M. Ginanneschi, F. Laschi, L. Messori, M. Muniz-Miranda, A. M. Papini, T. Kowalik-Jankowska and H. Kozłowski, *J. Inorg. Biochem.*, 2002, **89**, 181.
27 G. Pappalardo, G. Impellizzeri, R. P. Bonomo, T. Campagna, G. Grasso and M. G. Saita, *New J. Chem.*, 2002, **26**, 593.
28 H. Kozłowski, W. Bal, M. Dyba and T. Kowalik-Jankowska, *Coord. Chem. Rev.*, 1999, **184**, 319.
29 L. D. Pettit, J. E. Gregor and H. Kozłowski, *Persp. Bioinorg. Chem.*, 1991, **1**, 1.
30 P. Młynarz, D. Valensin, K. Kociolek, J. Zabrocki, J. Olejnik and H. Kozłowski, *New J. Chem.*, 2002, **26**, 264.